Structural Engineering and Mechanics, *Vol. 58, No. 2 (2016) 327-345*
DOI: http://dx.doi.org/10.12989/sem.2016.58.2.327

Chord rotation demand for effective catenary action of RC beams under gravitational loadings

Meng-Hao Tsai*

Department of Civil Engineering, National Pingtung University of Science and Technology, No.1 Hseuh-Fu Rd., Neipu, Pingtung County, 912 Taiwan

(Received October 27, 2015, Revised January 18, 2016, Accepted January 29, 2016)

Abstract. Many experimental and analytical studies have been conducted with beam-column sub-assemblages composed of a two-span beam to investigate the progressive collapse resistance of RC frames. Most study results reveal a strength-decreased transition phase in the nonlinear static load-deflection curve, which may induce dynamic snap-through response and increase the chord rotation demand for effective catenary action (ECA). In this study, the nonlinear static response is idealized as a piecewise linear curve and analytical pseudo-static response is derived for each linearized region to investigate the rotation demands for the ECA of the two-span RC beams. With analytical parameters determined from several published test results, numerical analysis results indicate that the rotation demand of 0.20 rad recommended in the design guidelines does not always guarantee the ECA. A higher rotation demand may be induced for the two-span beams designed with smaller span-to-depth ratios and it is better to use their peak arch resistance (PAR) as the collapse strength. A tensile reinforcement ratio not greater than 1.0% and a span-to-depth ratio not less than 7.0 are suggested for the two-span RC beams bridging the removed column if the ECA is expected for the collapse resistance. Also, complementary pseudo-static analysis is advised to verify the ECA under realistic dynamic column loss even though the static PAR is recovered in the nonlinear static response. A practical empirical formula is provided to estimate an approximate rotation demand for the ECA.

Keywords: progressive collapse; effective catenary action; pseudo-static response; chord rotation

1. Introduction

Progressive collapse vulnerability of building structures has been an active research topic since the 9/11 terrorist attack on the World Trade Center in 2001. As stated in the ASCE 7-10 Standard (ASCE 2010), progressive collapse is defined as "the spread of an initial local failure from element to element, resulting eventually in the collapse of an entire structure or a disproportionately large part of it" and sometimes indicated as "disproportional collapse". In fact, the origin of the progressive collapse research can be traced back to the partial collapse of the Ronan Point apartment building in 1968 (Pearson and Delatte 2005). The incident inspires the subsequent emphasis on the structural integrity and makes the prevention of progressive collapse an important issue in the development of several structural design codes (Mohamed 2006). Feasible engineering

*Corresponding author, Professor, E-mail: mhtsai@mail.npust.edu.tw

http://www.techno-press.org/?journal=sem&subpage=8 ISSN: 1225-4568 (Print), 1598-6217 (Online)

approaches for mitigating the risk of progressive collapse have been proposed and evaluated (Ellingwood 2006, Nair 2006). The U.S. General Service Administration (GSA 2003, 2013) and Department of Defense (DoD 2005, 2009, 2013) have issued detailed step-by-step design and analysis guidelines and conduct periodical review and modification. Extending from earlier analytical and numerical researches, many experimental studies for the progressive collapse have been carried out in the past decade. Load redistribution mechanisms for the column-loss response are investigated from field tests of real building structures (Sasani *et al*. 2007, Sasani 2008, Song and Sezen 2013). It is believed that most realistic dynamic column-loss behavior and valuable experimental data could be captured from the field tests of real structures. However, the opportunity for conducting such prototype structural tests depends on the willingness of the building owner and the cost could be very expensive as compared with reduced-scale model tests in laboratory. Besides, field tests of real building structures are non-repeatable and it is hard to get whatever structural response under different loading conditions.

Hence, most experimental studies concerning the progressive collapse resistance of building structures are conducted with frame models and beam-column sub-assemblages. Yi *et al* (2008) carried out a static experimental study with a four-bay and three-story one-third scale RC frame model to investigate the progressive collapse resistant behavior. Chen *et al*. (2012) used a full-scale two-story steel moment frame to evaluate the dynamic response under sudden column loss. As compared with the frame model tests, more tests have been done with the so called beam-column sub-assemblages, as shown in Fig. 1, to catch the progressive collapse behavior of the two-span beams. Su *et al*. (2009) performed static vertical loading tests on twelve longitudinally restrained two-span RC beams with varied steel and span-to-depth ratios. They indicated that the test specimens could reach the peak arch strength at a deflection ranging from 16% to 34% of the section depth. For some specimens, the load resistance in the catenary stage could be lower than the arch strength. Sasani *et al*. (2011) adopted a 3/8 scaled sub-assemblage to evaluate the column-loss response of a two-span RC beam bridging over a removed column. Choi and Kim (2011) performed static loading tests on reduced-scale RC sub-assemblages designed with and without seismic detailing and concluded that significant catenary action may be activated for seismically detailed beams. Yu and Tan (2013) designed eight RC sub-assemblage specimens with varied steel and span-to-depth ratios to study the ultimate catenary resistance under column loss. A series of scaled sub-assemblages were designed and tested to investigate the effects of slab on the collapse resistance under corner column loss (Qian and Li 2012a, 2013, 2015, Qian *et al*. 2015). Full-scale RC beam-column sub-assemblages with and without seismically designed details were tested by Lew *et al*. (2014). Tsai *et al*. (2014) evaluated the influence of different reinforcement layouts on the collapse-resistant behaviour of RC beams. Also, the effects of span-to-depth ratio and stirrup spacing on the collapse resistance were assessed in a later experimental study (Tsai and Chang 2015). Some dynamic tests have been carried out to investigate more realistic column-loss response of RC beam-column sub-assemblages and structural frames (Tian and Yu 2011, Qian and Li 2012b, Orton and Kirby 2014).

Most test results support that the catenary action may be used as the final defensive mechanism against collapse. It is also realized that development of the catenary action is dependent on the beam-end rotational capacity. The design guidelines issued by the GSA (2013) and DoD (2013) have proposed an acceptance criterion of 0.20 rad for the chord rotation capacity of the two-span beams, as indicated in Fig. 1, to ensure the development of catenary action. This threshold is specified independent of the member design parameters. However, from those referred experimental studies, the rotation demands for the catenary development may be different.

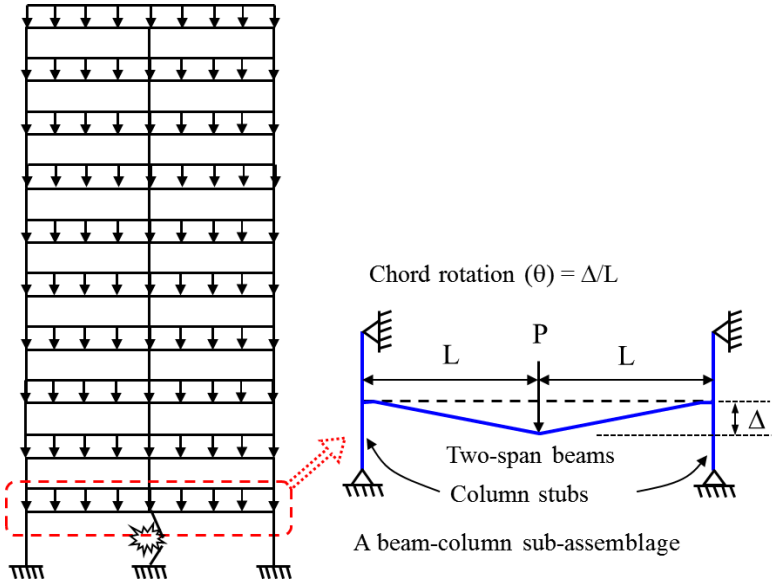

Fig. 1 The definition of a beam-column sub-assemblage

Therefore, analytical resolution of the rotation demands for effective catenary action (ECA) in progressive collapse analysis is proposed in this study. The ECA is defined as the recovery of peak arch resistance in the catenary phase. Piecewise linear curves divided by the yield strength, peak arch resistance (PAR), leveled off strength (LOS), and peak catenary resistance (PCR) before bar fracture are constructed to idealize the general nonlinear static response of the two-span RC beams under gravitationally monotonic loadings. Since the arch and catenary actions are not significant for the loss of a corner or a penultimate column, the scenario of interior- or middle-column loss is the main concern herein. Then, their corresponding pseudo-static responses are derived for each linearized region. The analytical expressions are used to conduct numerical investigations on the chord rotation demands of the ECA and associated snap-through response. With the analytical parameters determined from several referred experimental studies and numerical analysis results, practical considerations are provided for progressive collapse design and analysis of building structures.

2. Idealization of static response

Most static tests have revealed that the load-deflection responses of the two-span beams (Fig. 1) are highly nonlinear under gravitationally monotonic loadings. The nonlinear static response is initiated at the tensile cracking of concrete and grows significantly as the tensile reinforcement yields. Along with the flexural yielding, the load response gradually reaches the PAR, as shown by P_a in Fig. 2(a). This load-deflection range is defined as the "compressive arch phase". In this phase, compressive axial force is developed in the two-span beams due to the constraint provided by the end columns. After the PAR, there is usually a strength-decreased phase in which the axial compression decreases with increased vertical deflection of the beams. It is defined as the "transition phase". The load resistance can decrease down to the LOS, P_C, where the catenary

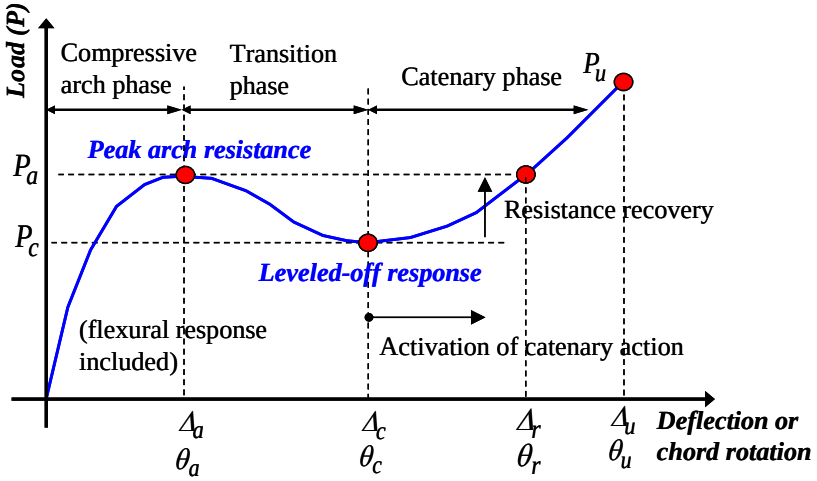

Fig. 2(a) Static load-deflection curve under gravitational monotonic loadings

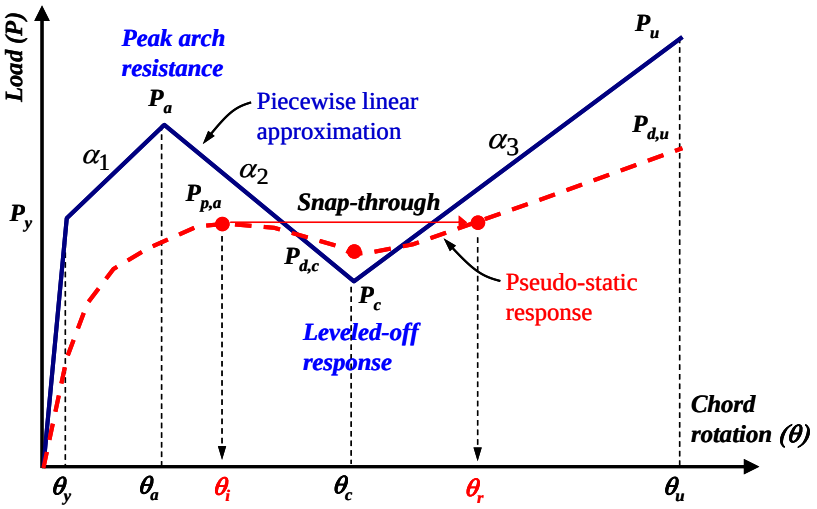

Fig. 2(b) Idealized piece-wise linear curve and pseudo-static response

action is activated. The LOS represents the resistance at the commencement of the catenary phase. (Sadek *et al*. 2011). This strength-decreased region may induce snap-through response under a real dynamic column-loss scenario (Tsai 2012, Orton and Kirby 2014). If the two-span beams have sufficient rotation capacity, the load resistance can be regained under the catenary action and even larger than the PAR before the rupture of any reinforcement. This region is thus defined as the "catenary phase". Axial tension is developed in the two-span beams during this phase and serves as ultimate resistance against collapse.

Although the general static load-deflection curve is nonlinear, as a rule of thumb, it can be approximated as a piece-wise linear curve with four threshold points, as shown in Fig. 2(b). The four threshold points are corresponding to the yielding strength, PAR, LOS, and PCR before bar fracture. As shown in the figure, the stiffness ratios of the three post-yield regions to the elastic

stiffness are designated by α_1, α_2, and α_3. α_1 is defined as the arch stiffness ratio ranging from the yield point to the PAR and expressed as

$$\alpha_1 = \frac{P_a - P_y}{P_y} \frac{\theta_y}{\theta_a - \theta_y}. \tag{1a}$$

Similarly, α_2 is defined as the softening stiffness ratio ranging from the PAR to the LOS. α_3 is defined as the catenary stiffness ratio for the catenary phase. They are respectively expressed as

$$\alpha_2 = \frac{P_a - P_c}{P_y} \frac{\theta_y}{\theta_c - \theta_a} \tag{1b}$$

and

$$\alpha_3 = \frac{P_u - P_c}{P_y} \frac{\theta_y}{\theta_u - \theta_c}. \tag{1c}$$

With these parameters, the analytical pseudo-static response in each phase can be obtained for the idealized nonlinear static response.

3. Analytical pseudo-static response

Static test results of the two-span RC beams cannot direct reflect the real dynamic column-loss response due to the exclusion of dynamic effect. Analytical and numerical studies (Tsai and Lin 2008, Tsai 2010, Tsai and You 2012) have indicated that the pseudo-static response obtained from the nonlinear static load-deflection curve can be used to predict the maximum dynamic response under column loss. Hence, they have to be transformed into their pseudo-static counterparts by using the equal work and energy method, as shown by the dash line in Fig. 2(b). This can be numerically implemented by dividing the accumulated area under the nonlinear static response curve by the corresponding displacement of the column-loss point and be expressed as

$$P_{CC}(u_d) = \frac{1}{u_d} \int_0^{u_d} P_{NS}(u) du \tag{2}$$

where P_{NS} (u) and P_{CC} (u) are, respectively, the nonlinear static loading and the pseudo-static counterpart at the displacement demand u. Therefore, for the idealized nonlinear static response, the pseudo-static resistance in the elastic range may be written as

$$P_{d,0} = P/2, \quad 0 \le P \le P_y \tag{3}$$

where P_y is the static yielding force. From the yield point to the PAR, the pseudo-static resistance $P_{d,1}$ is derived as

$$P_{d,1} = \frac{P_y[\alpha_1(\mu - 1)^2 + 2(\mu - 1) + 1]}{2\mu}, \quad 1 \le \mu \le \mu_a \tag{4}$$

where the ductility, μ, is the chord rotation divided by the yield rotation θ_y. μ_a is the ductility

demand at the PAR P_a (Fig. 2(b)) and equal to θ_a/θ_y. Similarly, the pseudo-static resistances in the transition and catenary phases are respectively derived as

$$P_{d,2} = \frac{P_{d,a}\mu_a}{\mu} + \frac{P_y[-\alpha_2(\mu-\mu_a)^2 + 2(\mu-\mu_a)[1+\alpha_1(\mu_a-1)]]}{2\mu}, \quad \mu_a \le \mu \le \mu_c \tag{5}$$

and

$$P_{d,3} = \frac{P_{d,c}\mu_c}{\mu} + \frac{P_y[\alpha_3(\mu-\mu_c)^2 + 2(\mu-\mu_c)[1+\alpha_1(\mu_a-1)-\alpha_2(\mu_c-\mu_a)]]}{2\mu}, \quad \mu_c \le \mu \tag{6}$$

where $P_{d,a}$=$P_{d,1}$ (μ=μ_a) and $P_{d,c}$=$P_{d,2}$ (μ=μ_C). μ_C is the ductility demand at the end of transition phase and equal to θ_C/θ_y. In fact, a general form for the pseudo-static resistance in the i-th linear region of a piece-wise linear curve with $i \geqq 2$ may be deduced from the above equations as

$$P_{d,i} = \frac{P_{d,i-1}(\mu_{i-1})\cdot\mu_{i-1}}{\mu} + \frac{P_y[\alpha_i(\mu-\mu_{i-1})^2 + 2(\mu-\mu_{i-1})[1+\sum_{j=1}^{i-1}\alpha_j(\mu_j-\mu_{j-1})]]}{2\mu}, \quad \mu_{i-1} \le \mu \tag{7}$$

where μ_{i-1} is the ductility demand of the previous turning point and the sign of stiffness is included in the stiffness ratios α_i and α_j.

As shown in Fig. 2(b), the pseudo-static PAR, denoted as $P_{p,a}$, does not occur at the chord rotation θ_a corresponding to its static counterpart. Instead, it happens during the transition phase, namely in the range from θ_a to θ_C. In fact, as the supported loading is larger than the pseudo-static PAR, the two-span beams could be loaded directly into the catenary phase and snap-through response may be induced under column loss and accompanied by significant deformation demand, as indicated in Fig. 2(b). Apparently, the pseudo-static PAR is critical to the snap-through behavior. From setting the derivative of Eq. (4) equal to zero, it can be obtained that $P_{p,a}$ occurs at

$$\mu \equiv \mu_i = \sqrt{\frac{(\alpha_2+2\alpha_1)\mu_a^2 + 2(1-\alpha_1)\mu_a - 2P_{d,a}\mu_a/P_y}{\alpha_2}} \tag{8}$$

The value of $P_{p,a}$ is then calculated as $P_{d,2}$ (μ=μ_i). The chord rotation at μ_i is denoted as θ_i in Fig. 2(b). This rotation is defined as the snap-through prevention limit and can be regarded as an index to judge the importance of the catenary action. If θ_i is larger than the expected beam-end rotation, the catenary action will be minor under the column loss. Moreover, from the comparison of the nonlinear static and pseudo-static load-deflection curves, it is clear that if the static leveled off rotation θ_C is less than θ_i, then the pseudo-static response presents a non-degrading curve with non-negative tangent stiffness. In such a case, there will be no snap-through response under dynamic column loss (Tsai 2012) and the collapse resistance is always larger than the pseudo-static PAR in the catenary phase. However, as θ_C is larger than θ_i, the pseudo-static resistance will be lower than $P_{p,a}$ and the snap-through response be induced consequently. Once this happens, the dynamically falling behavior can be arrested only if the resistance of $P_{p,a}$ may be regained in the catenary phase. Otherwise, dynamic collapse will happen. Therefore, an effective catenary action is defined as the capability of recovering the strength of $P_{p,a}$ in the catenary phase. The chord rotation demand for the effective catenary action is then determined from $P_{d,3} \geq P_{p,a}$, which leads to

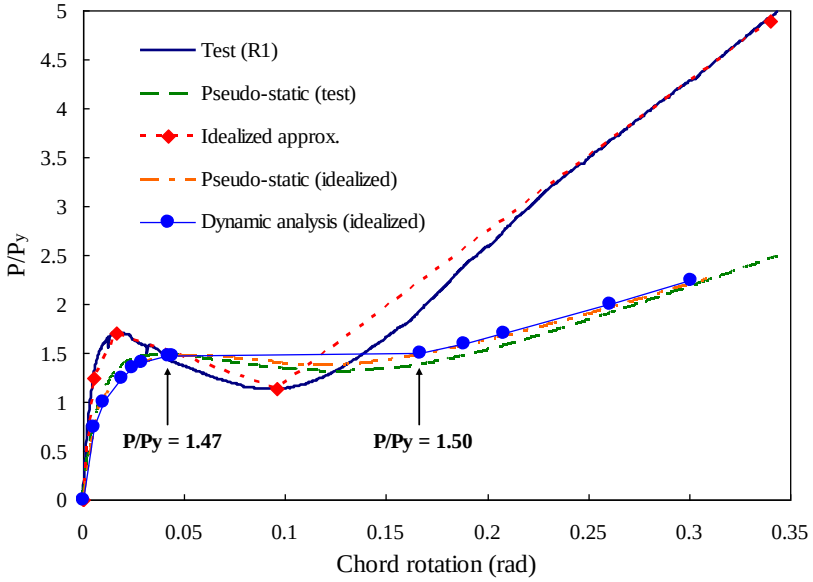

Fig. 3 Experimental and idealized static and pseudo-static response curves of the R1 specimen

$$A\mu^2 + B\mu + C \geq 0 \tag{9}$$

where

$$A = \alpha_3, \tag{10a}$$

$$B = 2[1 + \alpha_1(\mu_a - 1) - \alpha_2(\mu_c - \mu_a) - \alpha_3\mu_c - 2P_{p,a}/P_y], \tag{10b}$$

and

$$C = \alpha_3\mu_c^2 - 2\mu_c[1 + \alpha_1(\mu_a - 1) - \alpha_2(\mu_c - \mu_a) - 2P_{d,c}/P_y] \geq 0. \tag{10c}$$

Two values of ductility demand, μ, can be resolved from Eq. (9). The one larger than μ_C, denoted as μ_r, is the ductility demand for the effective catenary action. Its corresponding rotation is designated as θ_r in Fig. 2(b).

4. Demonstration

A test specimen adopted from Tsai and Chang (2015) is used as an example to demonstrate the approximation of the piece-wise linear curve to the nonlinear response. Design details of the specimen may be found in the referred literature. Fig. 3 presents its normalized static load and chord rotation response curve and the piece-wise linear approximation. The threshold values of the idealized approximation and the three corresponding stiffness ratios are summarized in Table 1. An equivalent single degree of freedom (SDOF) model has been constructed with the idealized approximation and its static response curve has been obtained from nonlinear pushdown analysis.

Table 1 Idealization parameters for the R1 specimen in Tsai and Chang (2015)

Phase	Compressive arch	Transition	Catenary
(P/P_y, θ)	(1.71, 0.0166)	(1.13, 0.0960)	(4.89, 0.340)
Stiffness ratio	α_1=0.16	α_2=0.029	α_3=0.062

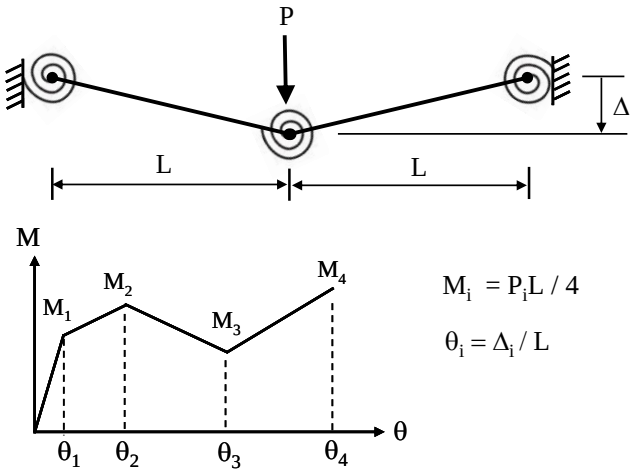

Fig. 4 The equivalent SDOF model and beam-end hinge properties

The SDOF model is composed of two prismatic beams with nonlinear hinges at the beam ends, as shown in Fig. 4. The idealized piece-wise linear hinge properties are determined from the static load-deflection response. It is defined as a SDOF model since it deforms in a single mode shape. The pseudo-static responses curves calculated from the test results and the numerical static response of the SDOF model are compared in the figure. It is seen that both pseudo-static curves were in good agreement. Using the analytical expressions with the parameters in Table 1 and the span-to-depth ratio, 8.0, of the test specimen, the chord rotations of snap-through prevention and ECA are estimated as θ_i=0.051 and θ_r=0.156 rad, respectively. They are approximate to 0.0538 and 0.164 rad, respectively, which are estimated from the pseudo-static analysis of equivalent SDOF model. This confirms that the analytical expressions can be used to estimate the chord rotations of snap-through prevention and ECA for the two-span RC beams under gravitational loadings. The snap-through induced chord rotation may be calculated as θ_r-θ_i with the analytical expressions. To demonstrate the existence of the snap-through response, incremental dynamic analyses of the SDOF model subjected to step loading functions with gradually increased magnitude have been carried out and the normalized response envelope is included in the figure. The inherent damping is neglected in the dynamic analysis. As indicated in the figure, an abruptly increase of the chord rotation demand is observed due to the snap-through behavior when the normalized loading is slightly increased from P/P_y=1.47 to P/P_y=1.50.

5. Parametric study

5.1 Determination of parameters

From the previous derivation, it is known that the chord rotation demand for the ECA is involved with several parameters, including the three stiffness ratios and chord rotations at the static peak arch and leveled off responses. These parameters are dependent on the span-to-depth ratio, reinforcement ratio, material strength, and constraints of the two-span beams bridging the removed column. The static test results of several published experimental studies (Su *et al*. 2009, Yu and Tan 2013, Lew *et al.* 2014, Tsai *et al*. 2014, Tsai and Chang 2015), as shown in Table 2, are used to evaluate the variations of these model parameters. For reducing the complexity of the evaluation, only those designed with continuous reinforcement and symmetric layouts and exhibiting catenary behavior (i.e. P_u>P_C in Fig. 2(b)) before any bar fracture are selected. The arch, softening, and catenary stiffness ratios are calculated by using the static peak arch, leveled off, and maximum catenary responses prior to bar fracture as listed in Table 2. The values for calculating the stiffness ratios are either obtained from the test results specified in the referred papers or estimated from the load-deflection curves if not specified.

Figs. 5(a) and 5(b) show the variations of α_1, α_2, and α_3 with respect to the span-to-depth ratios and averaged beam-end tensile reinforcement ratios, respectively. The span-to-depth ratio is varied between 4.0 and 11.0 and the reinforcement ratio between 0.61% and 1.34%. The reinforcement ratios are obtained from averaging the tensile steel ratios at the beam ends of those selected specimens. From Fig. 5(a), although the distribution is scattered, more or less, the arch and catenary stiffness ratios appear to increase with the span-to-depth ratios. However, no specific trend may be observed for the softening stiffness ratio. Similarly, scattered distribution with the tensile reinforcement ratio is observed in Fig. 5(b). It is seen that the arch and catenary stiffness ratios roughly increase with the steel ratio as the steel ratio is larger than 1.0%. Because of the scattered distribution, no curve fitting is conducted to relate the stiffness ratios with the span-to-depth ratio. Even though, the figures reveal that most of the stiffness ratios are varied from 0.1 to 0.2 for α_1, from 0.05 to 0.15 for α_2, and from 0.05 to 0.2 for α_3. Therefore, the stiffness ratios selected for the parametric study are determined as shown in Table 3.

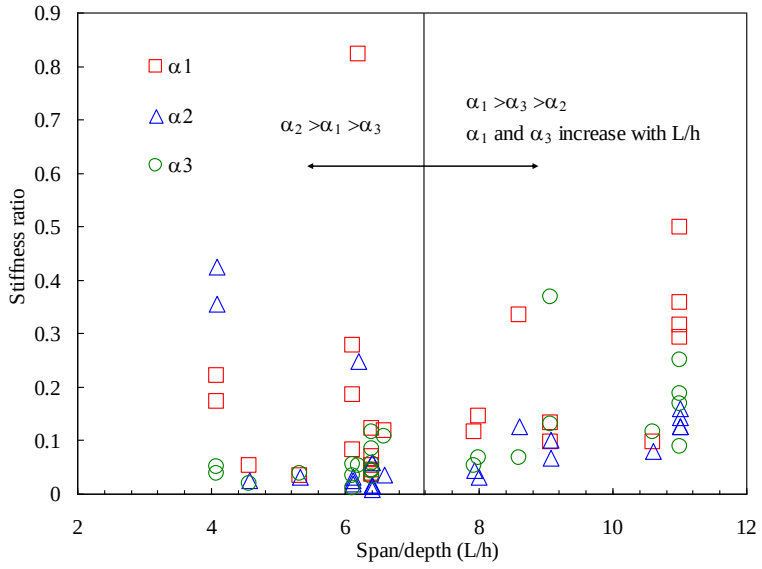

Fig. 5(a) Variation of the estimated stiffness ratios with the span-to-depth ratios

Table 2 Selected test results for analytical parameters of idealized piece-wise linear approximation

Referred studies	Specimen ID	Span/depth ratio	Yield point		Peak arch resistance		Leveled off strength		Peak catenary resistance	
			Load (kN)	Deflection (cm)	Load (kN)	Deflection (cm)	Load (kN)	Deflection (cm)	Load (kN)	Deflection (cm)
Yu and Tan (2013)	S2	11	29.0	3.47	38.4	7.30	19.3	25.23	39.1	37.87
	S4	11	47.8	4.25	63.2	8.10	47.8	16.71	59.2	28.30
	S5	11	56.6	5.01	70.3	7.45	51.6	20.54	94.9	43.39
	S6	11	62.0	8.01	70.3	11.44	63.0	18.12	93.0	33.71
	S7	8.6	61.1	3.60	82.8	7.44	58.0	19.00	65.4	25.41
	S8	6.2	84.7	3.01	121.3	4.59	75.2	11.18	92.0	22.50
Su *et al*. (2009)	A3	4.08	152.0	2.01	246.0	7.64	145.0	11.40	178.0	19.90
	A6	4.08	153.0	1.83	226.0	6.92	109.8	10.20	144.0	20.90
	B1	6.58	105.0	3.83	125.0	10.00	109.8	25.30	150.0	38.90
	B2	9.08	73.2	4.33	82.9	10.20	70.6	17.40	121.0	25.50
	B3	9.08	65.0	4.01	74.7	8.55	54.9	26.50	90.2	43.10
	C1	6.13	48.2	0.80	60.9	3.37	48.0	14.20	65.7	22.70
	C2	6.13	45.2	1.00	64.9	3.35	52.0	14.80	77.6	25.00
	C3	6.13	45.2	1.00	68.6	2.87	52.0	14.80	54.4	20.10
Lew *et al*. (2014)	IMF	10.60	267.0	6.00	296.0	12.70	196.0	40.60	547.0	109.20
	SMF	7.93	790.0	5.00	903.0	11.20	632.0	50.70	1232.0	121.90
Tsai *et al*. (2014)	S1	6.40	89.2	1.20	109.7	8.60	101.7	21.35	154.4	43.60
	S2	6.40	42.2	0.68	58.2	7.75	48.9	18.15	135.0	51.80
	S4	6.40	63.5	1.52	76.7	8.61	69.7	18.56	196.0	55.01
Tsai and Chang (2015)	R1	8.00	37.1	0.92	47.1	2.65	31.2	15.36	137.6	55.00
	R2	5.33	108.8	1.57	125.5	8.56	105.1	17.96	182.3	47.47
	R3	4.57	155.2	1.58	196.0	9.56	157.7	25.41	186.7	41.31
	R4	6.40	60.2	0.90	73.2	3.66	58.0	19.11	156.1	51.66
	SS1	6.40	60.3	2.48	71.3	6.21	56.9	16.11	166.1	55.01
	SS2	6.40	60.3	1.30	70.4	5.41	50.5	12.56	163.1	54.61

In addition to the stiffness ratios, the chord rotations at the static peak arch (θ_a) and leveled off (θ_C) responses are another two important parameters for constructing the idealized piece-wise linear curves. Fig. 6 shows the variation of these two chord rotations obtained from the referred experimental studies with respect to the span-to-depth ratios. It is observed that these two parameters have a more distinct trend with the span-to-depth ratio than the stiffness ratios. Hence, power regression has been conducted for them and the regression formulae are indicated in the figure. Although the coefficients of determination (R^2) in the figure reveal that the curve fitting results are not perfectly consistent with the test results, at least, the general trend of decreasing with increased span-to-depth ratios is confirmed for these two chord rotations. Therefore, the regression formulae

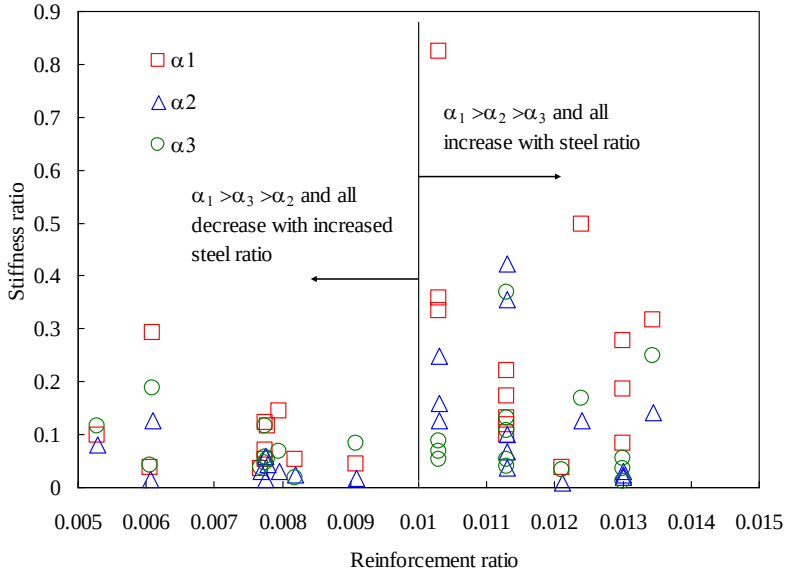

Fig. 5(b) Variation of the estimated stiffness ratios with tensile reinforcement ratios

Table 3 Stiffness ratios of the three phases for the parametric study

α_1	α_2	α_3
0.1	0.05 ~ 0.15 @ 0.05	0.05 ~ 0.2 @ 0.05
0.2	0.05 ~ 0.15 @ 0.05	0.05 ~ 0.2 @ 0.05

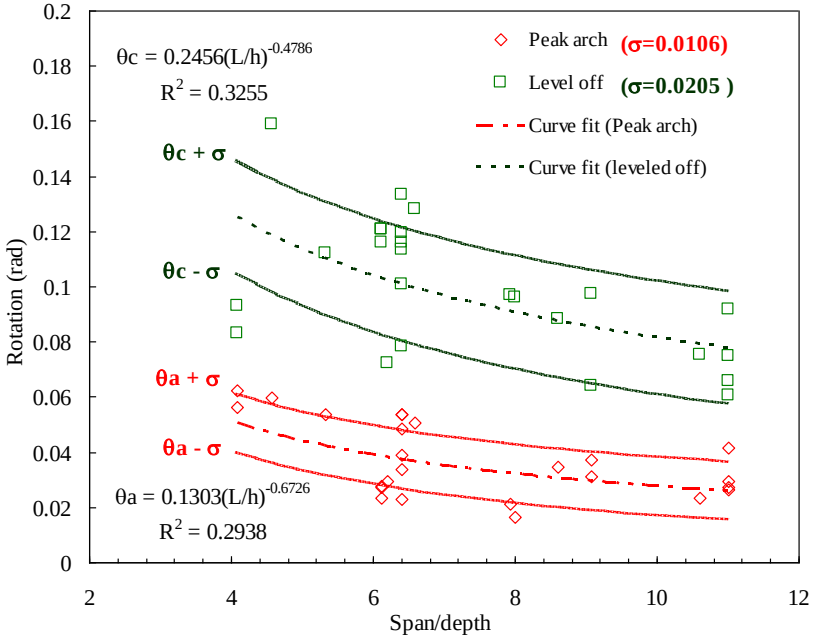

Fig. 6 Variation of θ_a and θ_C with span-to-depth ratios

$$\theta_a = 0.1303(L/h)^{-0.6726} \tag{11a}$$

and

$$\theta_C = 0.2456(L/h)^{-0.4786} \tag{11b}$$

are used to determine the rotation at the static PAR and LOS in the following numerical investigation. In the formulae, L is the clear length of a single span and h is the section depth. Standard deviations of the predicted θ_a and θ_C are equal to 0.0106 and 0.0205 rad, respectively. The predicted θ_a and θ_C with plus and minus one standard deviation are also presented in the figure. Then, with a given yield rotation θ_y, the ductility demands at the static PAR and LOS may be calculated and the aforementioned analytical pseudo-static response be determined as well.

5.2 Numerical investigation

Based on the analytical expressions and determined parameters, the chord rotation demands of the two-span RC beams under gravitational loadings are investigated in this section. Although there are 20 different combinations for the considered stiffness ratios, only typical results are presented herein for better clarification of their influence. Since the analytical derivation is carried out with rotational ductility, a yield rotation, denoted as θ_y in Fig. 2(b), should be provided for a quantitative evaluation. The beam-end yield rotation is usually assumed as 0.005 rad (FEMA 2000) in conventional nonlinear analysis. However, as estimated from the referred experimental studies, the average yield rotation is approximate to 0.01 rad. In order to clarify its effect on the rotation demand, numerical analyses with θ_y=0.005 and 0.01 rad have been conducted and compared. The comparison results indicate that the chord rotation demands with θ_y=0.005 rad are slightly larger than the other in a similar variation trend. Therefore, only the numerical investigations with θ_y=0.01 rad are presented in the following.

At first, the variations of the snap-through prevention rotation (θ_i) under five typical combinations of α_1 and α_2 are shown in Fig. 7. From Eq. (8), it is known that the catenary stiffness ratio does not contribute to this rotation. The equation reveals that θ_i increases with the static peak-arch rotation (θ_a). In other words, it would decrease with increased span-to-depth ratio, as shown in the figure. Also, a larger arch stiffness ratio and a smaller softening stiffness ratio would lead to a larger snap-through prevention rotation. Generally speaking, it is around 0.07±0.02 rad in the figure for the considered span-to-depth range. It is noted that the snap-through prevention rotations are larger than the collapse prevention level in the conventional performance-based seismic design (FEMA 2000). This explains why the acceptance criteria of plastic rotation for RC beams suggested in the GSA guidelines (GSA 2013) are around two times larger than that in the FEMA 356 guidelines. The development of catenary action would be minor if the chord rotation demand of the two-span beams is less than this snap-through prevention limit.

Fig. 8(a) shows the comparison of the minimum rotation demands (θ_r) for the ECA under five different parametric combinations with α_1=0.1. The corresponding snap-through response calculated as (θ_r-θ_i) is shown in Fig. 8(b). These figures reveal that, similar to the referred experimental results, the rotation demands of both the ECA and snap-through response decrease with increased span-to-depth ratio. With a larger softening stiffness ratio, for example α_2=0.1 and 0.15 in the figure, the rotation demand for the ECA would likely be larger than the prescribed 0.20 radians in the GSA and DoD guidelines. In other word, the criterion of 0.20 radians does not

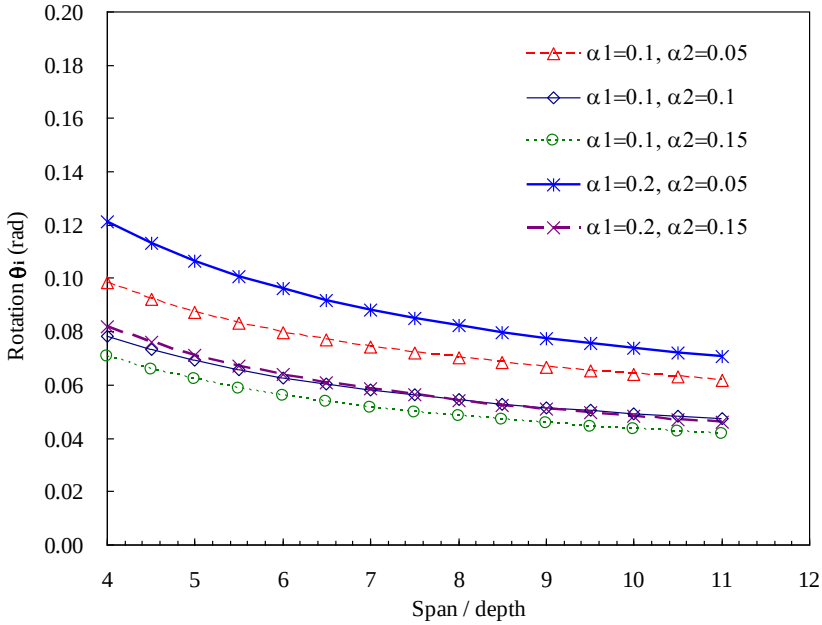

Fig. 7 Variation of snap-through prevention rotations

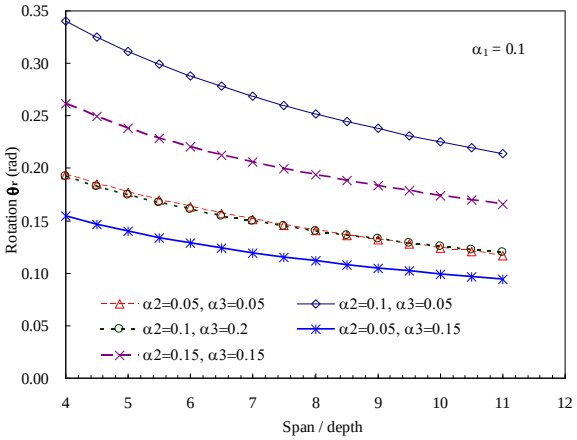

Fig. 8(a) Minimum rotation demands (θ_r) for effective catenary action with α_1=0.1

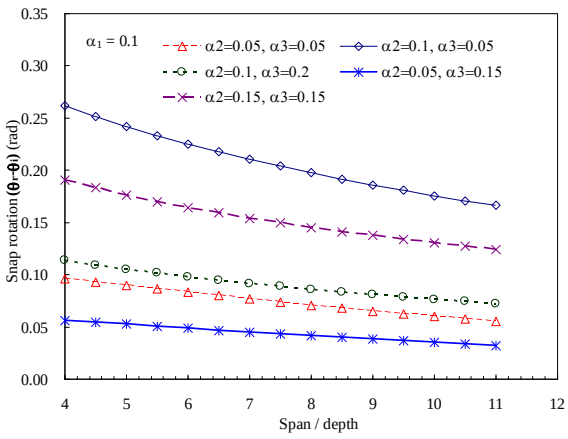

Fig. 8(b) Snap-through rotation (θ_r-θ_i) with α_1=0.1

always guarantee the ECA. A larger softening stiffness ratio, α_2, means swifter stiffness degradation in the transition phase and thus delays the recovery of PAR. It may occur in members suffered from shear failure during the gravitational monotonic loading process (Tsai and Chang2015). Also, as observed from the figures, it is realized that a significant portion of the rotation demand with a larger softening stiffness ratio is induced by the snap-through response.

It is seen in Fig. 8(a) that either increasing the catenary stiffness or decreasing the softening stiffness can help to reduce the rotation demands. Decreasing the softening stiffness ratio α_2 may

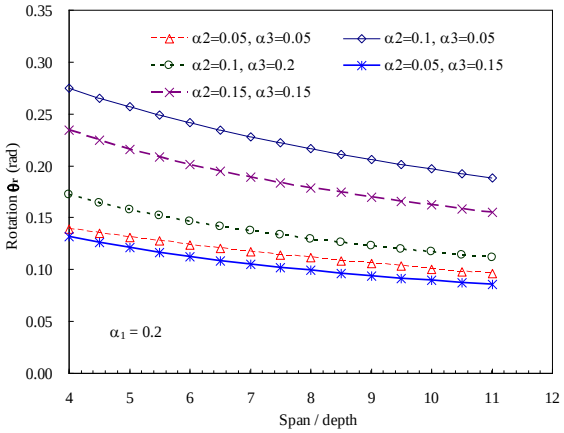

Fig. 9(a) Minimum rotation demands (θ_r) for effective catenary action with α_1=0.2

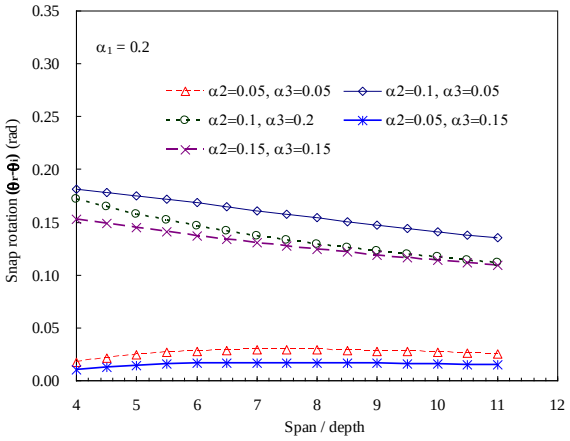

Fig. 9(b) Snap-through rotation (θ_r-θ_i) with α_1=0.2

be more beneficial than increasing the catenary stiffness ratio α_3 in the demand reduction. For example, similar reduction is achieved for the case of α_2=0.1 and α_3=0.05 by either reducing α_2 to 0.05 or increasing α_3 to 0.2. In Fig. 5(a), it is observed that the catenary stiffness ratio approximately increases with the span-to-depth ratio as the latter is larger than 7.0. In this range, the catenary stiffness ratio is generally larger than the softening stiffness ratio and thus benefits the rotation reduction. Also, α_3 is generally larger than α_2 when the averaged tensile reinforcement ratio is less than 1.0%, as shown in Fig. 5(b). These evidences imply that the chord rotation demand for the ECA under gravitational loading may be reduced if high tensile reinforcement ratio and deep-section design can be avoided for the two-span RC beams.

The influence of increasing arch stiffness ratio on the chord rotations of the ECA and snap-through response is shown in Fig. 9(a) and 9(b), respectively. Compared with Figs. 8(a) and 8(b), it is seen that a larger arch stiffness ratio may reduce both the rotation demands for the ECA and snap-through response. For a given span-to-depth ratio, an increased arch stiffness can result in larger static PAR and snap-through prevention limit, θ_i, as observed from Fig. 2(b) and Fig. 7. This will lead to a reduced strength degradation range, namely (θ_C-θ_i), and alleviate the strength degradation. It is especially apparent for the cases with smaller softening stiffness ratios, as shown by the curves with α_2=0.05 in Fig. 9(b), where the snap-through rotation has been significantly reduced. Also, an increased span-to-depth ratio may reduce the leveled off rotation θ_C as indicated by Eq. (11b) and increase the arch stiffness ratio as revealed in Fig. 5(a). Hence, earlier triggered catenary action may be expected for the two-span RC beams designed with a shallower section. Their PAR, denoted as $P_{p,a}$ in Fig. 2(b), can be recovered at a less chord rotation demand in the catenary phase.

5.3 Importance of pseudo-static analysis

Although dynamic tests can reflect the realistic column-loss scenarios, the experimental costs for test setup and instrumentation are usually higher than conventional static tests. Hence, there are more experimental studies conducted with static tests. Based on the idealized piece-wise linear

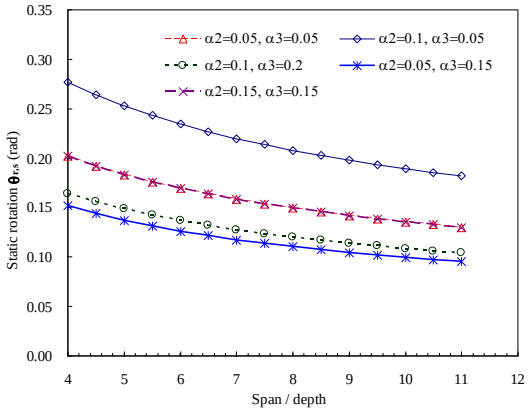

Fig. 10(a) Static rotation demands for the effective catenary action

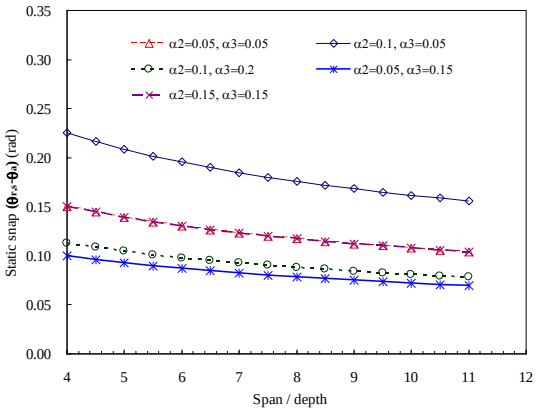

Fig. 10(b) Static rotation demands for the snap-through response

curve, a rotation demand for the static ECA can be obtained from setting P_a=P_u in Fig. 2(b). The resulting rotation, $\theta_{r,s}$, is written as

$$\theta_{r,s} = \theta_y \frac{(\alpha_2 + \alpha_3)\mu_c - \alpha_2 \mu_a}{\alpha_3} \tag{12}$$

Different from the pseudo-static rotation demand obtained from Eq. (9), the static rotation is independent of the arch stiffness ratio. Figs. 10(a) and 10(b) show the rotation demands for the static ECA and snap-through response based on Eq. (12). The comparison of Fig. 10 and Fig. 8 indicates that the rotation demands, either for the ECA or the snap-through response, may be underestimated by using the nonlinear static response. The larger the rotation demand is, the more significant the underestimation could be. Therefore, if the monotonic static test results of the two-span RC beams present a recovery of the PAR in the catenary phase, complementary pseudo-static analysis is necessary to verify the ECA under realistic dynamic column loss.

5.4 Practical consideration

5.4.1 Design parameters

From the parametric numerical investigation, it is known that a larger span-to-depth ratio, larger arch and catenary stiffness ratios, and smaller softening stiffness ratio are beneficial for the reduction of rotation demands. Hence, it would be favorable if the two-span beams may be designed to achieve this goal. From Fig. 5(b), it appears that the minimum arch and catenary stiffness ratios occur around an averaged reinforcement ratio of 1.0%. As the averaged reinforcement ratio ($\rho_{s,avg}$) is less than 1.0%, the arch stiffness ratio would be generally larger than the other two ratios and the softening stiffness ratio be the smallest one and remain approximately constant. This implies that a tensile steel ratio not larger than 1.0% would be better for less rotation demand for the ECA. On the contrary, if $\rho_{s,avg}$ is larger than 1.0%, the stiffness ratios appear to increase with the reinforcement ratio and both the arch and softening stiffness ratios may be comparable and larger than the catenary stiffness ratio. As revealed from the parametric study, this would induce a larger rotation demand for the ECA. Similar observation from Fig. 5(a) indicates

that a span-to-depth ratio larger than 7.0 would be better for smaller rotation demand for the ECA since the softening stiffness ratio is smaller than the other two in this range. Therefore, a tensile reinforcement ratio not larger than 1.0% and a span-to-depth ratio not less than 7.0 are suggested for the two-span RC beams bridging over the removed column if catenary action is expected in the collapse resistance.

5.4.2 Generalized empirical formula

From the figures of the rotation demand for the ECA, it is known that it may be expressed as a power function of the span-to-depth ratio. Hence, an empirical formula is proposed as

$$\theta_r = A(\frac{L}{h})^B \tag{13}$$

where A and B are the undetermined coefficients. Using the parametric study results, the undetermined coefficients A and B have been obtained for each rotation demand curve. They are approximated with linear functions of the three stiffness ratios as

$$A = a_0 + a_1\alpha_1 + a_2\alpha_2 + a_3\alpha_3 \tag{14a}$$

$$B = b_0 + b_1\alpha_1 + b_2\alpha_2 + b_3\alpha_3 \tag{14b}$$

where a_i and b_i with i= 0~3 are the regression coefficients. Least-square fit is carried out for the twenty sets of coefficients to find the optimal A and B. The final results give

$$A = 0.4786 - 1.093\alpha_1 + 2.377\alpha_2 - 1.149\alpha_3 \tag{15a}$$

$$B = -0.5526 + 0.7370\alpha_1 + 0.3092\alpha_2 - 0.2069\alpha_3 \tag{15b}$$

Corresponding to Figs. 8(a) and 9(a), the rotation demands for the ECA predicted by using the empirical formulae are shown in Figs. 11(a) and 11(b), respectively. From the comparison of the figures, it is known that accuracy of the empirical formulae is acceptable in most cases. Therefore, instead of the derived rigorous analytical expressions, the empirical formulae may be used to

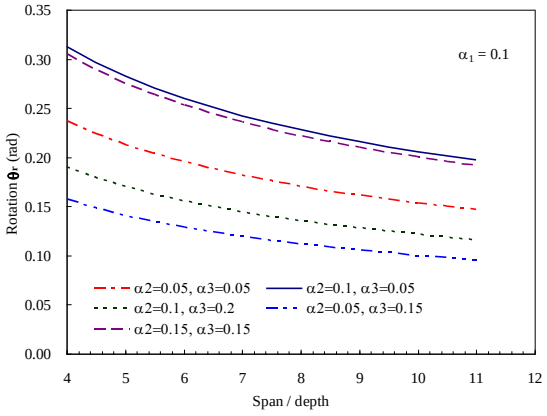

Fig. 11(a) Predicted rotation demand of effective catenary action with α_1=0.1

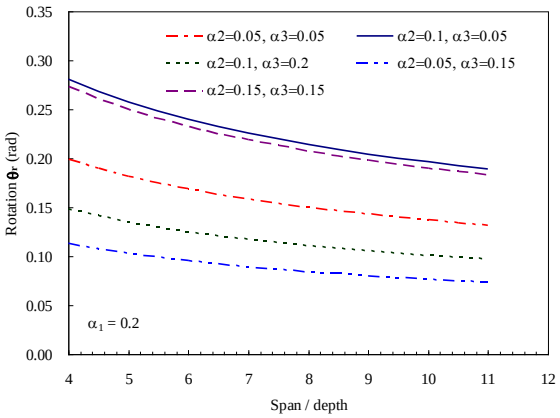

Fig. 11(b) Predicted rotation demand of effective catenary action with α_1=0.2

estimate an approximate rotation demand for the ECA of the two-span RC beams under column loss.

6. Conclusions

Because of the widespread attention paid to the progressive collapse resistance of building structures under column loss in the past decade, several experimental studies have been performed with beam-column sub-assemblages composed of a two-span beam. Most test results reveal that the development of catenary action is dependent on the beam-end rotational capacity. Hence, chord rotation demands for effective catenary action (ECA) of the two-span RC beams are investigated in this study. The ECA is defined as the recovery of the peak arch resistance (PAR) in the catenary phase. The nonlinear static response of the two-span RC beams under monotonic gravitational loadings is idealized as a piece-wise linear curve characterized by the yield strength, PAR, leveled off strength, and peak catenary resistance before bar fracture. Arch, softening, and catenary stiffness ratios are defined for the post-yield stiffness of the corresponding linearized region. Based on the idealized static response, analytical formulations are derived to determine the rotation demands for the ECA and snap-through response. Static test results of several published experimental studies are used to determine the analytical parameters for the numerical parametric study. The study results reveal that the rotation demand of 0.20 rad recommended in the GSA and DoD guidelines for catenary development does not always guarantee the ECA. A larger rotation demand for the ECA may be induced if the span-to-depth ratio of the two-span RC beams decreases. Also, increasing the arch and catenary stiffness ratios and decreasing the softening stiffness ratio are beneficial to the reduction of rotation demands. Because of a larger span-to-depth ratio, earlier triggered ECA may be expected for the two-span beams designed with a shallow section. On the contrary, higher rotation demands may be induced for those designed with a deep section. Since RC members with a deep section are usually responsible of large shear and/or moment demands, it is thus suggested to use their PAR, instead of the ultimate catenary strength, as the progressive collapse resistance for safety concern. The snap-through prevention limit, which is the rotation demand at the PAR, approximately varies between 0.05 rad and 0.10 rad for the considered span-to-depth range. Furthermore, the rotation demand for the ECA may be underestimated by using the nonlinear static response. Thus, complementary pseudo-static analysis is advised to verify the ECA under realistic dynamic column loss even if the static PAR can be recovered in the nonlinear static response. From the variations of the analytical parameters estimated from the referred experimental studies and the parametric study results, a tensile reinforcement ratio not greater than 1.0% and a span-to-depth ratio not less than 7.0 are suggested for the two-span RC beams bridging over the removed column if the ECA is expected in the collapse resistance. Instead of the rigorous analytical expressions, the proposed empirical formula is practical for estimating an approximate rotation demand for the ECA of the two-span RC beams.

Acknowledgments

This study was supported by the National Science Council of Taiwan through grant No. MOST 103-2221-E-020-011. The support is gratefully acknowledged.

References

ASCE (2010), *Minimum Design Loads for Buildings and Other Structures, ASCE/SEI 7-10*, American Society of Civil Engineers, Reston, Virginia.

Chen, J., Huang, X., Ma, R. and He, M. (2012), "Experimental study on the progressive collapse resistance of a two-story steel moment frame", *J. Perform. Constr. Facil.*, ASCE, **26**(5), 567-575.

DoD, Department of Defense (2005), *Design of Buildings to Resist Progressive Collapse, UFC 4-023-03*, Washington, DC, USA.

DoD, Department of Defense (2009), *Design of Buildings to Resist Progressive Collapse, UFC 4-023-03*, Washington, DC, USA.

DoD, Department of Defense (2013), *Design of Buildings to Resist Progressive Collapse, UFC 4-023-03*, Washington, DC, USA.

Ellingwood, B.R. (2006), "Mitigating risk from abnormal loads and progressive collapse", *J. Perform. Constr. Facil.*, ASCE, **20**(4), 315-323.

FEMA (2000), *Prestandard and Commentary for the Seismic Rehabilitation of Buildings, FEMA-356*, Federal Emergency Management Agency, Washington, DC, USA.

GSA, General Service Administration (2003), *Progressive Collapse Analysis and Design Guidelines for New Federal Office Buildings and Major Modernization Projects*, Washington, DC, USA.

GSA, General Service Administration (2013), *Alternate Path Analysis & Design Guidelines for Progressive Collapse Resistance*, Washington, DC, USA.

Lew, H.S., Bao, Y., Pujol, S. and Sozen, M.A. (2014), "Experimental study of reinforced concrete assemblages under column removal scenarios", *ACI Struct. J.*, **111**(4), 881-892.

Mohamed, O.A. (2006), "Progressive collapse of structures: annotated bibliography and comparison of codes and standards", *J. Perform. Constr. Facil.*, ASCE, **20**(4), 418-425.

Nair, R.S. (2006), "Preventing disproportionate collapse", *J. Perform. Constr. Facil.*, ASCE, **20**(4), 309-314.

Orton, S. and Kirby, J. (2014), "Dynamic response of an RC frame under column removal", *J. Perform. Constr. Facil.*, ASCE, **28**(4), 04014010-1-8.

Pearson, C. and Delatte, N. (2005), "Ronan Point apartment tower collapse and its effect on building codes", *J. Perform. Constr. Facil.*, ASCE, **19**(2), 172-177.

Qian, K. and Li, B. (2012a). "Slab effects on response of reinforced concrete substructures after loss of corner column", *ACI Struct. J.*, **109**(6), 845-855.

Qian, K. and Li, B. (2012b), "Dynamic performance of reinforced concrete beam-column substructures under the scenario of the loss of a corner column-experimental results", *Eng. Struct.*, **42**, 154-167.

Qian, K. and Li, B. (2013), "Experimental study of drop-panel effects on response of reinforced concrete flat slabs after loss of corner column", *ACI Struct. J.*, **110**(2), 319-330.

Qian, K. and Li, B. (2015), "Quantification of slab influences on the dynamic performance of RC frames against progressive collapse", *J. Perform. Constr. Facil.*, ASCE, **29**(1), 04014029-1-11.

Qian, K., Li, B. and Ma, J. (2015), "Load-carrying mechanism to resist progressive collapse of RC buildings", *J. Struct. Eng.*, **141**(2), 04014107-1-14.

Sasani, M., Werner, A. and Kazemi, A. (2011), "Bar fracture modelling in progressive collapse analysis of reinforced concrete structures", *Eng. Struct.*, **33**, 401-409.

Sasani, M., Bazan, M. and Sagiroglu, S. (2007), "Experimental and analytical progressive collapse evaluation of actual reinforced concrete structures", *ACI Struct. J.*, **104**(6), 731-739.

Sasani, M. (2008), "Response of a reinforced concrete infilled-frame structure to removal of two adjacent columns", *Eng. Struct.*, **30**, 2478-2491.

Song, B.I. and Sezen, H. (2013), "Experimental and analytical progressive collapse assessment of a steel frame building", *Eng. Struct.*, **56**, 664-672.

Su, Y., Tian, Y. and Song, X. (2009), "Progressive collapse resistance of axially-restrained frame beams", *ACI Struct. J.*, **106**(5), 600-607.

Tian, Y. and Su, Y. (2011), "Dynamic response of reinforced concrete beams following instantaneous

removal of a bearing column", *Int. J. Concrete Struct. Mater.*, **5**(1), 19-28.
Tsai, M.H. and Lin, B.H. (2008), "Investigation of progressive collapse resistance and inelastic response for an earthquake-resistant RC building subjected to column failure", *Eng. Struct.*, **30**, 3619-3628.
Tsai, M.H. (2010), "An analytical methodology for the dynamic amplification factor in progressive collapse evaluation of building structures", *Mech. Res. Commun.*, **37**, 61-66.
Tsai, M.H. (2012), "A performance-based design approach for retrofitting regular building frames with steel braces against sudden column loss", *J. Constr. Steel Res.*, **77**, 1-11.
Tsai, M.H. and You, Z.K. (2012), "Experimental evaluation of inelastic dynamic amplification factors for progressive collapse analysis under sudden support loss", *Mech. Res. Commun.*, **40**, 56-62.
Tsai, M.H., Lu, J.K. and Huang, B.H. (2014), "Column-loss response of RC beam-column sub-assemblages with different bar-cutoff patterns", *Struct. Eng. Mech.*, **49**(6), 775-792.
Tsai, M.H. and Chang, Y.T. (2015), "Collapse-resistant performance of RC beam-column sub-assemblages with varied section depth and stirrup spacing", *Struct. Des. Tall Spec. Build.*, **24**, 555-570.
Yi, W.J., He, Q.F., Xiao, Y. and Kunnath, S.K. (2008), "Experimental study on progressive collapse-resistant behavior of reinforced concrete frame structures", *ACI Struct. J.*, **105**(4), 433-439.
Yu, J. and Tan, K.H. (2013), "Structural behaviour of RC beam-column sub-assemblages under a middle column removal scenario", *J. Struct. Eng.*, ASCE, **139**(2), 233-250.

CC